PAPER • OPEN ACCESS

Frequency dependence of the speed of sound in metallic rods

To cite this article: A Marques and M S Rodrigues 2023 *Phys. Scr.* **98** 126101

Physica Scripta

PAPER

Frequency dependence of the speed of sound in metallic rods

A Marques[1,2] and M S Rodrigues[1,3]

[1] Departamento de Física, Faculdade de Ciências, Universidade de Lisboa, Portugal
[2] CENIMAT/I3N, Departamento de Ciência dos Materiais, Faculdade de Ciências e Tecnologia, Universidade Nova de Lisboa, Caparica, 2829-516, Portugal
[3] Biosystems & Integrative Sciences Institute, Faculdade de Ciências, Universidade de Lisboa, Lisboa, Portugal

E-mail: msrodrigues@fc.ul.pt

Keywords: sound speed, standing wave, thin rod, Pochhammer-Chree dispersion

OPEN ACCESS

RECEIVED
6 June 2023

REVISED
7 September 2023

ACCEPTED FOR PUBLICATION
24 October 2023

PUBLISHED
3 November 2023

Abstract

The speed of sound waves in rods depends on the relationship between wavelength and rod dimensions. It differs from the speeds readily available in tables, and from what is often learned during most introductory courses on solid-state physics. Metallic rods with diameters in the centimetre range excited with sound waves of tens of kHz will behave as dispersive media. Here, the speed of sound in metallic titanium rods of different lengths is measured using two different methodologies: (1) from the time of flight and (2) from the wavelength and frequency of standing waves that form in the rod. The latter allows analyzing the results in light of Pochhammer-Cree dispersion. The reflection coefficient is also determined both from time and from frequency response. Two off-the-shelf piezoelectric transducers, a function generator, an oscilloscope, and a lock-in amplifier were used. We have used a low-frequency square wave (of tens of Hz) in the first case and a sine wave with frequencies that range from audible to ultrasound in the second case. Experimental results show that the speed of sound decreases as the wavelength decreases. The Pochhammer-Chree dispersion equation was numerically solved to fit the experimental data that can be used to estimate both the Young modulus and the Poisson ratio. A practical empirical formula that allows data analysis without explicitly solving the Pochhammer-Chree equation is suggested.

1. Introduction

Here, we explore the speed of sound in metallic rods, aiming to provide practical insights to a broad academic audience, including non-graduates. We've simplified the theoretical framework to enhance accessibility, emphasizing conventional experimental techniques that can be used to measure sound speed and associated mechanical properties. Additionally, we introduce a practical empirical formula to analyze data, avoiding explicitly solving the Pochhammer-Chree equation. This helps explain dispersive effects in thin metallic rods, particularly how sound speed varies with frequency and object dimensions, with applications in engineering and materials science. Sound is a mechanical pressure wave in which motion is described as the transport of energy and momentum from one point in space to another without the transport of matter. As a sound wave travels it causes the continuous displacement of the atoms from their rest or equilibrium positions [1]. These waves can be said to be composed of phonons such as electromagnetic waves can be decomposed into photons. Phonons, the quantum analogue of photons, are units of vibrational energy arising from the atomic oscillations and travelling at the speed of sound. The oscillation of the atoms can either be parallel or perpendicular to the wave's direction of propagation. These two polarisations propagate at different speeds and are called longitudinal and transverse waves respectively. Because air cannot withstand shear, sound is a longitudinal wave. For small disturbances, one can picture a solid as a collection of atoms of mass m connected by massless springs of stiffness k, in the so-called harmonic approximation. The spring constant being the negative of the second derivative of the interatomic potential energy.

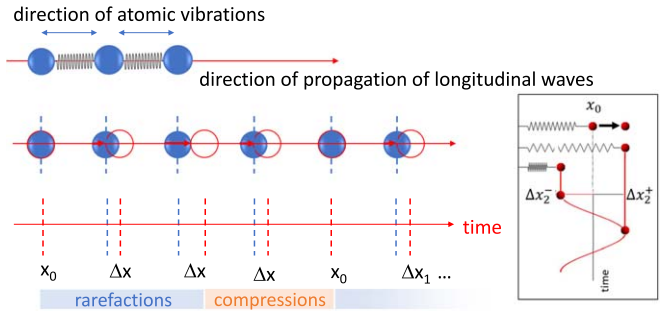

Figure 1. Longitudinal wave propagation in a solid in the spring ball model, where balls represent the atoms and springs the interatomic force gradients.

A rod can be thought of as a collection of thin disks connected by as many springs as there are atoms on the surface of each disk. If the wavelength is much larger than the diameter of the disk, then pressure differences occur at scales larger than the radius of the disks, meaning that these individually keep their overall form. When longitudinal waves propagate under these circumstances they are called extensional waves (the fundamental mode corresponding to a modulation of the length of the rod). The number of springs connecting the disks is proportional to the disk surface area A and so is the stiffness. The total deformation of the rod is the sum of the excess separation between two adjacent disks times the number of disks that compose the rod. Thus, for a given force F the deformation of the bar is proportional to its length L. Hence, the rod stiffness is:

$$\frac{F}{\Delta L} = \frac{A}{L}E \tag{1}$$

Where E is the Young modulus that can be expressed as the ratio of the pressure F/A, called stress, to the relative deformation $\Delta l/l$, called engineering strain [2]. In simple materials like metals, the Young modulus relates directly to the *springs* connecting individual atoms, each spring having a value which is given by the Young modulus times the separation between atoms. In materials like polymers, the young modulus depends on the degree of disorganization, or entropy of the system [2].

Another material property that we need to introduce is the Poisson ratio ν which relates to the tendency a material has to maintain its volume when its length is modified. Materials, that like rubber, when stretched decrease their cross-sectional area maintaining the volume constant have $\nu \approx 0.5$, whereas materials like cork, have $\nu \approx 0$ and keep their length despite, for instance, the increase in cross-sectional area that occurs when removed from a bottle. For most materials $0 < \nu < 0.5$ and for metals $\nu \approx 0.3$. The Poisson ratio is approximately given by the ratio of how much a material deforms say dl in the y and z directions $dl = dy = dz$ when stretched along the x-axis by an amount dx:

$$\nu \approx -\frac{dL}{dx} \tag{2}$$

The negative signal means, that if one dimension increases the other two usually decrease.

The speed of sound waves is a function of the Young modulus and of the Poisson ratio, but under common circumstances it also depends on the relationship between wavelength and the object's dimensions. It differs from the speeds readily available in tables, and from what is taught during most introductory courses on solid-state physics. While dispersion due to the sound wavelength being comparable to interatomic spacing is usually addressed, dispersion due to the dimensions of the object is not so commonly addressed. In the literature, the subject is addressed mostly in the context of the Hopkinson bar [3, 4]. The rod radius' considered here range from $r << \lambda$ (speed of extensional waves) to $r \approx \lambda$ where dispersion (see below) must be considered.

In the laboratory experiment proposed here, a piezoelectric transducer is put to vibrate with simple harmonic motion at an angular frequency ω, or excited with a step function, in a direction parallel to the axis of the rod. In the first simpler case, the piezoelectric dithering causes the atoms of the rod to oscillate with simple harmonic motion about their equilibrium positions mostly in the longitudinal direction. As the atoms get closer to neighbouring atoms, each atom transmits its momentum to its neighbours at a rate that provides the velocity of propagation of compression and rarefaction disturbances as illustrated in figure 1. In the last case, the impulse, which can be thought to contain a continuum of all frequencies, travels through the rod, and because each frequency component travels at a different speed the pulse shape evolves to a new shape [5, 6]; the medium is dispersive. In the limit of a thin rod ($\lambda >> L$) the extensional and transverse waves propagate at speeds given by:

$$v_e = \sqrt{\frac{E}{\rho}} \tag{3}$$

$$v_t = \sqrt{\frac{G}{\rho}} \tag{4}$$

where G is the shear modulus and it can be written as $G = E/2(1 + \nu)$. By measuring the speed of both waves and knowing the mass of the rod it is possible to determine E, G and ν. These speeds, given by the equations above, are very easy to find in tables. However, as we shall see, the actual speeds at which mechanical waves propagate can be relatively different.

1.1. Energy loss

The attenuation of sound for a wave with amplitude A at a position x is described as an exponential decay (see also figure 4) of its intensity, which is in turn directly proportional to the square of its amplitude:

$$A(x)^2 = A_0^2 \, \mathrm{e}^{-\alpha x} \tag{5}$$

where A_0 is the initial amplitude of the wave and α the attenuation coefficient. Each time the wave travels the length L of the rod, the wave intensity is reduced by a factor $exp[-\alpha L]$. If a fraction R of the incident intensity is reflected back at the rod's end, and then back again at the other end, and so on, the amplitude of the wave after each reflection is:

$$\begin{aligned} A_1^2 &= A_0^2 R e^{-\alpha L} \\ A_2^2 &= A_1^2 R e^{-\alpha L} = A_0^2 (R e^{-\alpha L})^2 \\ A_3^2 &= A_0^2 (R e^{-\alpha L})^3 \\ A_n^2 &= A_0^2 (R e^{-\alpha L})^n \end{aligned}$$

Where n corresponds to the n^{th} reflection which occurs at time $t = n\Delta T$, ΔT being the time it takes for the wave to travel the length L of the rod. Hence, taking into account $n = t/\Delta T$, using $a^b = e^{b \ln(a)}$, and taking the square root, the set of equations above can be approximated to a time-continuous equation:

$$A(t) = A_0 e^{-t(\frac{-ln(R)}{2\Delta T} + \frac{\alpha L}{2\Delta T})} \tag{6}$$

Sound waves in metals can travel several kilometres, which implies that the absorption of energy in a rod of only a few centimetres can be neglected. If we set α equal to 0 we obtain:

$$A(t) = A_0 e^{-\frac{t}{2\tau}} \tag{7}$$

with

$$\tau = -\frac{\Delta T}{\ln(R)} \tag{8}$$

This time constant is associated with energy loss and can also be determined from the frequency spectrum as we note below. It also follows, of course, that because absorption is negligible, the transmission coefficient is simply given by: $T = 1 - R$. The acoustic impedance can be used to estimate how much of the incident sound intensity is reflected back to the medium and how much is transmitted into the second medium. The acoustic impedance of a material is a measure of how much it opposes the displacement caused by sound waves and it is given by:

$$Z_0 = c\rho \tag{9}$$

where ρ is the density of the material and c is the speed of sound in that material. When a wave reaches the boundary between two materials with different impedance, part of the energy is reflected and part is transmitted. The transmission coefficient is given by:

$$T = \frac{I_T}{I_0} = \frac{4Z_1 Z_2}{(Z_1 + Z_2)^2} \tag{10}$$

where Z_1 and Z_2 are the media impedance. The signal reflected at an interface is given by

$$R = \frac{I_R}{I_0} = \frac{(Z_1 - Z_2)^2}{(Z_1 + Z_2)^2} \tag{11}$$

For metals, c is of the order of a few thousand m/s and ρ of the order of several thousand kg m^{-3}, so the impedance of a metal is likely above the 10 MPa s m^{-1}. Air on the other hand is much less dense and the speed of sound is only about 330 m s^{-1}. Hence one expects that most of the energy is reflected at the rod's end. Of course, here the amount of energy lost does not depend on the impedance of the media because some of the energy is lost as kinetic energy to the actuators attached to each of the rod's ends.

1.2. Standing waves

The reflection of the sound waves at each extremity of the rod will cause interference that can either be constructive or destructive depending on whether the displacement carried by waves arriving from the left cancels or adds to the displacement carried by waves coming from the right. For interference to be constructive the time it takes for the wave to go from left to right and come back again must exactly match an integer number of periods. In other words, for a given confined space such as a rod, there are certain frequencies for which this interference results in a stationary vibration pattern called a standing wave. When the wavelength equals twice the length of the rod, then when the first wave has travelled the distance $2L$ (forward and back) and is again reflected at the boundary, it will be in phase with a second wave generated at the piezoelectric emitter boundary and as a result, a large amplitude wave builds up in the rod. In general, the resonance will occur if the distance $2L$ is any integer times the wavelength. Therefore, the condition for resonance is:

$$2L = n\lambda \tag{12}$$

where n is any integer. This may be re-written in terms of the frequency of the waves, by replacing λ by c/f:

$$f_n = \frac{c}{2L}n \tag{13}$$

Plotting the intensity of the wave as a function of frequency should result in several peaks at the frequencies given above. The relative height and width of each peak depend on the reflection coefficient. The larger the reflection coefficient the more waves interfere constructively. Since the sum is maximized at the exact frequency the addition of more waves also causes the peaks to become thinner. However, because the piezoelectrics used to excite and detect the waves have their own transfer functions, the amplitude of the peaks is not a practical measure of the energy lost away, but the width of the peaks is. We can assume that in a range small enough around each peak the actuator-sensor transfer functions are approximately constant. It can be seen that the peaks are Lorentzian-like, as are those of a harmonic oscillator with resonance frequency satisfying equation 13 and as in a harmonic oscillator, the width of the Lorentzian is related to the decay time τ of the oscillator, i.e to the rate at which energy is lost away, which in turn is related to the reflection coefficient as given by equation 8.

$$A = \frac{A_{\max}}{\sqrt{\Delta f^2 \quad + \quad 4(f - f_n)^2}} \tag{14}$$

If we square the amplitude measured we obtain a signal proportional to the intensity of the wave. The full width at half maximum (FWHM) of the A^2 curve is given by:

$$\Delta f = \frac{1}{2\pi\tau} \tag{15}$$

1.3. Dispersion

In non-dispersive media, the wave speed does not depend on the frequency. Generally speaking, all media become dispersive for wavelengths sufficiently small. For unbounded media dispersion sets, as wavelength approaches inter-atomic spacing, typically at frequencies above the THz, however, in a finite solid, dispersion sets in much quicker, as soon as the wavelength becomes comparable to the object's dimensions. For instance, in a rod, radial inertia and wave interaction with the cylinder surfaces must be considered. Radial inertia is caused by the kinetic energy of the wave following radially outward as the rod is compressed. The wave that reaches the rod's surface is slightly retarded relative to the wave at the centre, but the distance between the centre of the rod's cross section and the surface is too small (much smaller than the wavelength) so that these two perturbations are coupled (the two waves are not independent) resulting in a wave that is slowed down dragged by the retarded wave. The first calculation of the elastic wave velocity in cylindrical rods was performed by L. Pochhammer [6–12].

The frequency equation, often termed the Pochhammer-Chree equation [6], can be simplified to take the following form [11] which is known as the Bancroft version of the Pochhammer-Chree equation:

$$(x - 1)^2\phi(hr) - (\beta x - 1)(x - \phi(kr)) = 0 \tag{16}$$

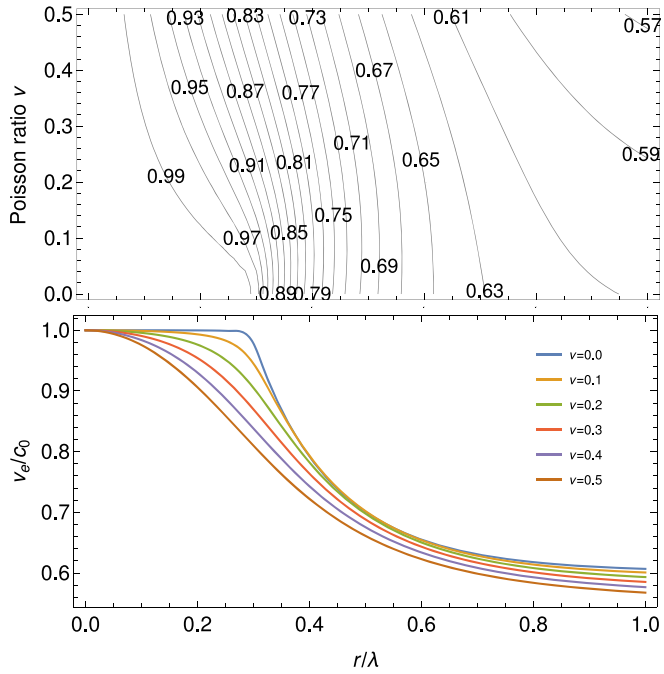

Figure 2. Ratio of actual sound speed of extensional waves to the conventional sound speed, v_e/c_0. Waves of wavelengths comparable to the radius of the rod travel slower than waves for which the wavelength is much larger than the rod's radius.

With

$$
\begin{aligned}
c_0 &= \sqrt{\frac{E}{\rho}} \\
x &= (1+\nu)\left(\frac{c_p}{c_0}\right)^2 \\
\beta &= \frac{1-2\nu}{1-\nu} \\
k &= \frac{2\pi}{\lambda}\sqrt{2x-1} \\
h &= \frac{2\pi}{\lambda}\sqrt{\beta x-1}
\end{aligned}
\tag{17}
$$

Where r, c_0, c_p, ν, λ, and E are respectively the rod radius, the longitudinal wave velocity (actual speed), the extensional wave velocity (conventional c_p=v_e), the Poisson's ratio, the wavelength, the Young modulus, and $\phi()$ is a Bessel function of the first kind. Since its proposal several solving algorithms [13] have been developed and used in several experiments that study the stress-strain state of materials caused by elastic waves, such as in the Hopkinson bar [3, 4].

Figure 2 clearly shows that in a finite rod of diameter, r the speed of sound strongly depends on the wavelength λ. By inferring the wavelength from the length of the rod and knowing its radius one can use figure 2 to estimate both the velocity of sound extensional waves $c = v_e$ and the Poisson ratio ν of the material and from the velocity, one can estimate the Young elasticity modulus E (equation 3). In the results section we provide an empirical formula (equation 19) that approximates well the solution of the Pochhammer-Chree equation.

Modelling wave propagation, including dispersion, is essential across various applications, spanning fields such as plasma physics, solid-state physics, optical fibres, chaos theory and more [14–17].

2. Materials and methods

Ti rods with a radius of 7.0 mm and 10 cm, 20 cm and 40 cm long were used. The rods were held by one lab stand holder as shown in figure 3. The speed of sound was determined using two different methodologies. The first one, the time of flight (TOF) relayed on the relationship between distance and time (i.e. $v = \frac{\Delta x}{\Delta t}$). A waveform generator (BK precision 4054B) was used for exciting a piezoelectric transducer (MCUSD14A40S09RS, of 40 kHz centre frequency) working as the emitter of sound waves, i.e. as a pressure wave generator. The emitter was

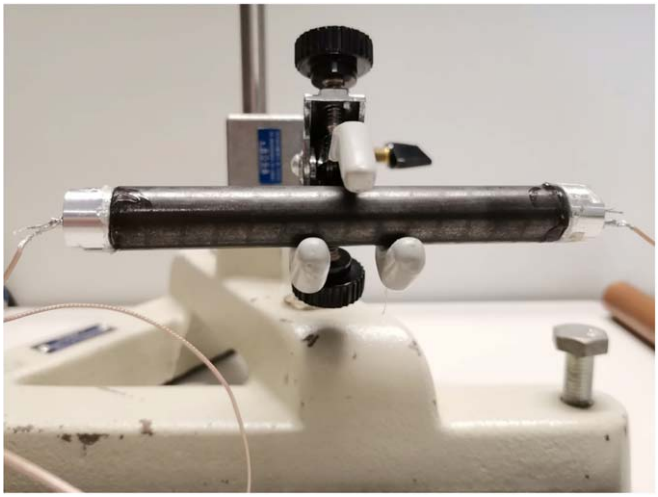

Figure 3. Photo of the lab stand holder with the 40 cm long Ti rod and piezoelectric transducers ultrasound gel coupled to its ends.

held at one end of the rod with ultrasound gel, and at the other opposed end, a second transducer of the same type was used as a receiver converting the sound pressure waves into electrical signals. The receiver output signal was displayed in an oscilloscope together with the incident wave input signal whose shape, frequency and amplitude were previously tuned at the waveform generator. A low-frequency square wave of 30 Hz was used.

The second method for determining the speed of sound in the rods is based on the wavelength and frequency of the standing wave (Eq. 13) and can also be implemented with the same materials by simply changing the excitation signal from a step function to a sinusoidal function. One can, of course, use the oscilloscope, however, it is faster explored using a lock-in amplifier and provides an opportunity for introducing it.

2.1. lock-in amplifier principle

We restrict this short hint to linear systems and assume the lock-in excites it with a sinusoidal stimulus at a well-defined reference frequency. The system's response $u(t)$ can be described as a background $B(\omega, t)$, due to noise, plus a component at the lock-in reference frequency that must come with some phase difference ϕ (response occurs after excitation). Thus, the signal at the input of the lock-in is of the form:

$$u(t) = R\sin(\omega_0 t - \phi) + B(\omega, t) \tag{18}$$

where R is the traditional letter used to represent the amplitude of the component at the lock-in frequency and should not be confused with the reflection coefficient. Assume care enough was taken to choose a frequency that is not present in the background. The lock-in amplifier multiplies the signal by $\sin(\omega_0 t)$ and in parallel it also multiplies the signal by $\cos(\omega_0 t)$. These multiplications will always result in products of sin and cos functions. Considering the multiplication by $\sin(\omega_0 t)$:

$$\begin{aligned} u(t)\sin(\omega_0 t) &= R\sin(\omega_0 t - \phi)\sin(\omega_0 t) + B(\omega, t)\sin(\omega_0 t) \\ &= R\cos(\phi)\sin(\omega_0 t)^2 \\ &\quad - R\sin(\omega_0 t)\cos(\omega_0 t)\sin(\phi) \\ &\quad + B(\omega, t)\sin(\omega_0 t) \end{aligned}$$

and similarly to the multiplication by $\cos(\omega_0 t)$. Then the trick is to average both results in time and note that the squares of the sin and cos functions can be written as a constant plus a term that oscillates with double frequency (e.g. $\sin(\omega t)^2 = 1/2 - \cos(2\omega t)/2$). Hence, averaging for long enough will cause the oscillatory terms to vanish. We are, thus, left with just the constant parts, which give respectively for the sin and cos multiplications:

$$\begin{aligned} \frac{R}{2}\cos(\phi) &\equiv \frac{x}{2} \\ -\frac{R}{2}\sin(\phi) &\equiv \frac{y}{2} \end{aligned}$$

Here, x and y are the letters traditionally used to represent the in-phase and in-quadrature components of the signal. Naturally, this result can only be obtained in the limit where the average takes forever, in practice a time constant is chosen so the average eliminates enough noise but still does not consume too much time. The lock-in can then use these vectors x and y to compute the amplitude R and the phase delay ϕ. This is similar to how radios can lock into a specific radio station despite receiving signals from many other radio stations and/or noise

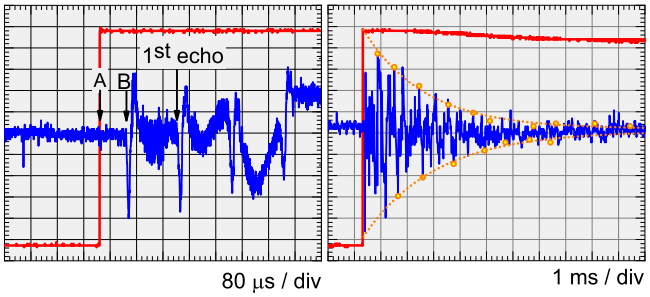

Figure 4. Emitted (red square wave) and received (blue) waves showing the instants (A), (B) and 1st echo corresponding to departure, arrival and arrival once again. The time delay between (A) and (B) corresponds to the time it takes the wave to travel once through the rod. The time delay between (B) and 1st echo corresponds to the time it takes a round trip.

sources. Because of its power to isolate/lock-in into a specific reference frequency, the lock-in can be used to detect very small signals and is a common tool in physics laboratories. Finally, by scanning the reference frequency one can evaluate the response of the system as a function of frequency.

3. Results and discussion

3.1. Method 1: time domain

The method based on the travelled distance L of a sound wave in a time interval Δt, or the time of flight, for determining the speed of sound is illustrated with the experimental data taken for the rod 40 cm long. Being the emitter transducer excited by a low-frequency square wave shape of 30 Hz. Note that the piezoelectric cannot actually alter the position of the rod in a step-wise manner, hence, the piezoelectric must recoil as it expands, in the process 'kicking' the rod much like a Dirac delta—one edge of the step function pushes and relaxes while at the other edge the piezoelectric pulls and relaxes. It is important to stress that the frequency must be low enough to enable the detection of the first reflection (one trip), and subsequent reflections (many trips) allowing the intensity of the wave to decrease substantially (due to sound being emitted away from the rod), before another wave is emitted. This means that the period of the wave must be longer than the amplitude decay time τ. The incident and received waves are shown in Fig. 4 in red and blue respectively. During each half period of the square wave, several reflections are observed in the oscilloscope.

The time interval corresponding to the sound wave propagation along the metallic rod length (L) was measured between points (A) and (B) (Δt_{AB}, ~0.08 ms). After point (B), a sequence of equidistant echo pulses with amplitude decreasing over time is observed. The echo sequence results from multiple sound wave reflections at the rod's end until all of its energy has leaked away to the exterior. The time between two consecutive echo pulses corresponds to a travelled distance of $2L$ and the first echo is detected after the time that a sound wave takes to travel a distance equal to three times the length of the rod ($3L$).

Now using for convenience, the time of 0.08 ms, measured on the rod 40 cm long, and the relationship $c = L/\Delta t$, one can determine the speed of sound in Ti to be ~5000 m/s, which only deviates 1.8 % of the reported value 5090 m/s [18]. This speed corresponds to the extensional wave speed (equation 3). Occasionally (on slightly larger rods), a small signal arrives before the signal corresponding to the extensional wave speed. If the piezoelectric is sufficiently fast to produce waves of a small enough wavelength (smaller than the rod's diameter), these can travel faster at the speed of longitudinal waves, and a small signal may be observed. The accuracy of this method is in any case improved if a digital oscilloscope can be used. Since by using its cursor tools and saving data option in a waveform format file, one can post-process the data. Accurately determining the time intervals is key.

All results are compiled in table 1. The reflection coefficient R was also extracted from the data shown in figure 4, acquired from the rod 40 cm long. As referred, this R-coefficient describes how much of a sound wave is reflected by an impedance discontinuity in the transmission medium, and can be determined by fitting an exponential envelope function (equation 6) to the measured signal. This is shown in figure 4, where the upper envelope and its symmetrical (lower envelope) are plotted with orange doted-lines. Both provided similar decay constants (i.e. ≈1.2 ms) and hence, similar reflection coefficients of ≈93 %. Aqueous ultrasound gel at the transducer/rod interfaces improves sound wave transmission across media [6]. The presence of an actuator and sensor, i.e. of the two identical piezoelectrics slightly alter the dynamics of the bar and are the main sources of error. Slight differences of about 1% may be observed by, for instance, moving the detector around.

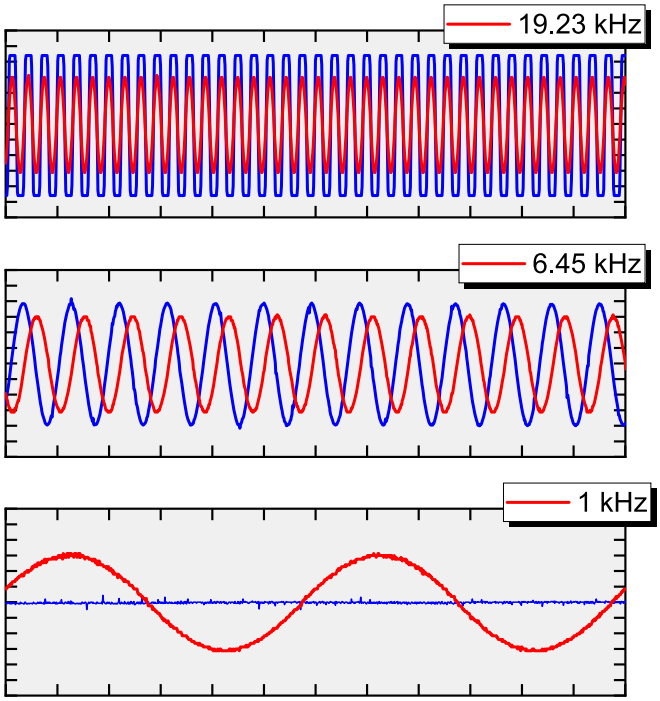

Figure 5. Excitation signal (red) and response (blue) at 19.23 k Hz and 6.45 kHz showing constructive interference and at 1 kHz showing negligible response. The vertical scale is the same in all plots.

Table 1. Values for the sound speed in m s^{-1} of extensional waves v_e transversal waves v_t obtained from the time of flight (TOF) and from the condition for the formation of standing waves (std-wave) and Poisson ratio obtained from adjusting the Pochammer-Chree equation (std-wave PC) and from the relationship between the speeds of both polarisation (longitudinal/transversal). Reference values [18] are 5090 m s^{-1} and 3125 m s^{-1} for extensional and shear waves respectively.

Length	9.95 cm	20.10 cm	49.95 cm
v_e (TOF)	5103	5180	5090
v_e (std-wave)	5078	5132	5127
v_t (std-wave)	3170	3168	—
ν (std-wave PC)	0.300	0.305	0.294
ν (v_e, v_t)	0.28	0.31	—

3.2. Method 2: frequency domain

The speed of sound can also determine for specific frequencies using the relationship $c = \lambda f$. This methodology makes clear Pochhammer-Chree dispersion that occurs in the rod when the wavelength approaches the radius of the bar. The first mode appears for a wavelength equal to twice the bar's length ($\lambda = 2L$), and it corresponds to a modulation of the actual length of the bar. The frequency that corresponds to this situation can be estimated from the speed of sound measured before. As shown in figure 5, the formation of the standing wave can readily be observed in the oscilloscope since at that specific frequency the observed signal is amplified.

The fastest and simpler way is if one lock-in amplifier is available. One can then perform a frequency sweep from a lower to an upper frequency and obtain the different modes in a single plot. It may well turn out that besides the extensional modes also the transverse modes are observed, particularly after the ultrasound gel has dried out (the wet gel decreases shear between the actuator and the bar). If transverse waves can be detected then the first two peaks should correspond to the first transverse mode and to the first extensional mode. From these two different velocities, we can estimate the Young and Shear modulus and from these the Poisson ratio. In figure 6 we show the frequency response for each of the three titanium bars. Some small peaks can also be observed that correspond to transverse waves. From the peaks marked 1 and 2 and using the expressions above

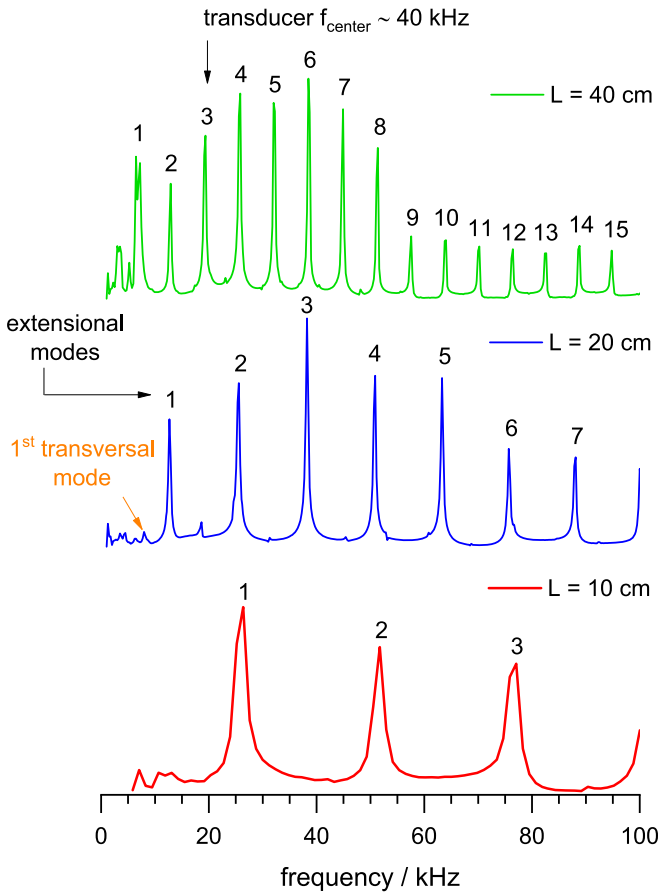

Figure 6. Amplitude of the harmonic signal captured at the detector as a function of frequency, measured with a lock-in amplifier.

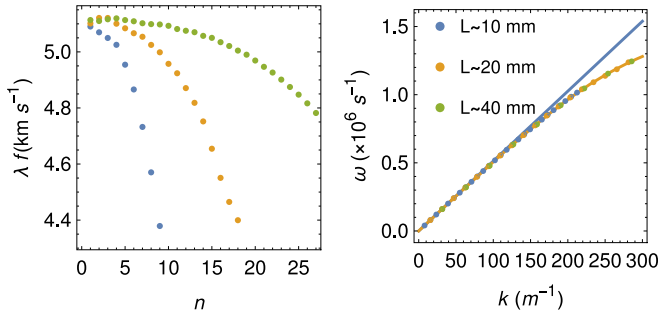

Figure 7. Experimental sound speed (wavelength times frequency $v = \lambda f$) as a function of mode number for all three titanium rods (left), and angular velocity as a function of wavenumber k (right). Waves of larger wave vectors travel slower through the rod.

we readily conclude $\nu = 0.3$. Using bars of different lengths one can compare the behaviour of sound waves of similar wavelengths, on different-length rods.

The 2nd mode on the 10 cm rod has the same wavelength as the 4th mode on the 20 cm rod and the 8th mode on the 40 cm rod (the longest rod is 4 times longer than the shortest and hence allows 4 times more modes). For all these three modes the wavelength is $\lambda = 10$ cm, and even though all three are affected by dispersion the determined sound speed is fairly identical, showing that the measured dispersion does not come from the rod's length. For all three bars, we observe that the distance between peaks is slowly reducing.

For each of the three bars and for each resonance mode one can calculate the speed of sound c using equation 13. In figure 7 we show how the velocity seems to depend on the mode number.

We can use figures 2 to estimate the Poisson ratio. This is illustrated in figure 8. If one knows the radius of the bar and the wavelength which is given by the length of the bar and n then one can calculate the amount r/λ, if the

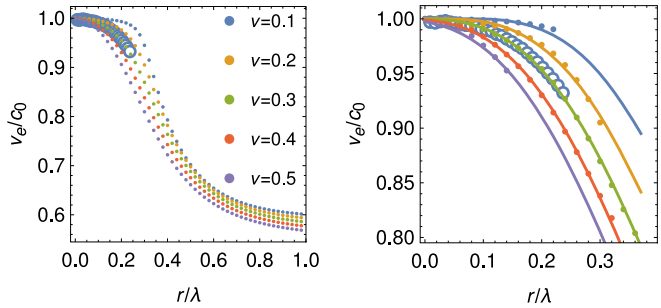

Figure 8. Numerical solutions of the Pochhammer-Chree equation are shown for different Poisson ratios as dots, and experimental data as open circles in both plots. Approximations given by equation 19 are shown as solid lines on the right panel, showing the agreement between the empirical formula 19 and the numerical solutions of the Pochammer-Cree equation 16.

bar length is several times the bar radius then the velocity obtained for the first modes can be used to normalize the velocities and compute the quantity c/c_p.

The experimental data superimposed on figure 2 can be used to give a rough estimate of the Poisson ratio. Alternatively the Pochhammer-Chree dispersion data shown in figure 2 can be fitted to a practical model to obtain an empirical formula:

$$\frac{c}{c_0} = \frac{1 + (a_1(\nu - \nu_0)^3 + a_3)(x + x_0)^3}{1 + (a_2(\nu - \nu_0)^3 + a_4)(x + x_0)^3} \tag{19}$$

With $a_1 = -282.29$, $a_2 = -326.28$, $\nu_0 = 0.3909$, a_3=4.500, a_4=10.130 and $x_0 = 0.3080(\nu - 0.2617)$ and x corresponding to the ratio given by the bar radius r divided by the wavelength λ, where λ is given by equation 12. Figure 8 shows this approximation together with the numerical solutions of equation 16. The equation above covers the range of the experiments presented here. Within the limits represented by solid dots in the right panel of figure 8, the maximum discrepancy is about 0.5%.This covers a wide range of materials, radius' and wavelengths. This formula fitted to the data of figure 8 yields c = 5118 m s^{-1} and $\nu = 0.3$. Finally, by analysing the Lorentzian-shaped peaks one can infer widths that vary from $\Delta f = 80$ Hz to about $\Delta f = 400$ Hz, the most common value being 140 Hz. As we stated before the width of the Lorentzian curve is associated with how energy flows from the system, hence, to the time constant τ and the reflection coefficient R. One must note, however, that the reflection varies with the gel being wetter/drier and also depends on the dynamics of the emitter-receiver transducer. That is, the reflection coefficient does not reflect the reflection from the solid to air, but rather the overall setup. To improve the measurement between the solid and air one should reduce the footprint of the sensors. Nonetheless, this results in time constants that vary from 400 μs up to 1.9 ms and is thus consistent with the signals observed in the oscilloscope ($\tau_{oscilloscope} \approx 1$ ms). This results in reflection coefficients that vary from R=0.9 up to R=0.98. Note that when obtaining the time constant from the oscilloscope, the slower decaying components superimpose on the faster decaying ones.

4. Conclusion

In conclusion, we have explored an experimental setup composed of one metallic bar, two piezoelectric actuators, one oscilloscope and optionally a lock-in amplifier. We have calculated the speed of sound from the time delay (time of flight) and by establishing standing waves in the bar. The main source of error is associated with the presence of the two piezoelectric actuators. Nonetheless, the results obtained differ by a maximum of 1.8 % from commonly accepted values [18]. Otherwise, the errors are associated with the precision in measuring length L, time delay ΔT and resonance frequency f_n of a particular mode n. These three variables connect directly to the sound speed c, since $c = L/\Delta T$ (method 1) and $c = 2Lf_n/n$ (method 2).

The time delay experiment results in a speed which is essentially the speed of extensional waves whereas the standing waves are sensitive to the dispersion that occurs when the wavelength approaches the bar radius. We have varied the wavelength from about 20r where dispersion is not visible down to about 3r where the speed of sound is clearly affected by dispersion. Additionally, we also discuss how to obtain the reflection coefficient by analysing either the time delay process, or by analysing the width of the peaks centred around each stationary mode. To simplify the analysis of experiments in which standing waves are established i.e. the wavelength is comparable to the bar's cross-sectional radius we suggest an empirical equation that very well approaches the results obtained from the much more calculus-intensive Pochhammer-Chree equation.

Data availability statement

The data cannot be made publicly available upon publication because they are not available in a format that is sufficiently accessible or reusable by other researchers. The data that support the findings of this study are available upon reasonable request from the authors.

ORCID iDs

A Marques https://orcid.org/0000-0002-6449-1537
M S Rodrigues https://orcid.org/0000-0002-0468-1910

References

[1] Meyers M A 1994 *Dynamic Behavior of Materials* (Wiley) vol 1 (https://doi.org/10.1002/9780470172278)
[2] Meyers M A and Chawla K K 2009 *Mecanical behavior of materials* vol 1 (Cambridge University Press)
[3] Shin H 2022 *J. Appl. Mech.* **89** 061007
[4] Barr A, Rigby S and Clayton M 2020 *Int. J. Impact Eng.* **139** 103526
[5] Marais S, Tait R, Cloete T and Nurick G 2004 *Latin American Journal of Solids and Structures* **1** 319–39
[6] Rigby S, Barr A and Clayton M 2017 *Proceedings of the Institution of Civil Engineers—Engineering and Computational Mechanics* **171** 1–21
[7] Pochhammer L 1876 *J. Reine Angew. Math.* **89** 324–36
[8] Chree C 1886 *The Quarterly Journal of Pure and Applied Mathematics* **21** 287–98
[9] Chree C 1889 *Trans. Cambridge Philos. Soc.* **14** 250–309
[10] Love A E H 1927 *Mathematical theory of elasticity* (Cambridge university press)
[11] Bancroft D 1941 *Phys. Rev.* **59** 588
[12] Mokryakov V 2019 *Procedia Structural Integrity* **23** 143–8
[13] Shin H 2022 *Proc. Inst. Mech. Eng. Part C J. Mech. Eng. Sci.* **236** 80–7
[14] Aly R, Seadawy D K and Chakrabarty A K 2018 *The European Physical Journal Plus* **133** 182
[15] Seadawy A R, Iqbal M and Lu D 2020 *Physica A* **544** 123560
[16] Seadawy A R, Rizvi S T R, Ahmad S, Younis M and Baleanu D 2021 *Open Physics* **19** 1–10
[17] Ahmad H, Seadawy A R and Khan T A 2020 *Phys. Scr.* **95** 045210
[18] Lide D R 2003 *CRC Handbook of Chemistry and Physics* (CRC Press)